

J. E. Sargison · M. L. G. Oldfield · S. M. Guo  
G. D. Lock · A. J. Rawlinson

## Flow visualisation of the external flow from a converging slot-hole film-cooling geometry

Received: 2 April 2003 / Accepted: 21 June 2004 / Published online: 26 January 2005  
© Springer-Verlag 2005

**Abstract** This paper presents flow visualisation experiments for a novel film-cooling hole, the converging slot-hole or *console* for short. Previously published experimental results have demonstrated that the *console* improved both the heat transfer and the aerodynamic performance of turbine vane and rotor blade cooling systems. Flow visualisation data for a row of *consoles* were compared with that of cylindrical and fan-shaped holes and a slot at the same inclination angle of 35° to the surface, on a large-scale, flat-plate model at engine-representative Reynolds numbers in a low speed tunnel with ambient temperature mainstream flow. In the first set of experiments, the flow was visualised by using a fine nylon mesh covered with thermochromic liquid crystals, allowing the measurement of gas temperature contours in planes perpendicular to the flow. This data demonstrated that the *console* film was similar to a slot film, and remained thin and attached to the surface for the coolant-to-mainstream momentum flux ratios of 1.1 to 40 and for a case with no crossflow (infinite momentum flux ratio). A second set of flow visualisation experiments using water/dry-ice fog have confirmed these results and have shown that the flow through all coolant geometries is unsteady.

J. E. Sargison  
School of Engineering, University of Tasmania,  
Tasmania, Australia

M. L. G. Oldfield  
Department of Engineering Science,  
University of Oxford, Oxford, UK

S. M. Guo  
Department of Mechanical,  
Aerospace and Manufacturing Engineering, UMIST,  
Manchester, UK

G. D. Lock (✉)  
Department of Mechanical Engineering,  
University of Bath, Bath, BA2 7AY, UK  
E-mail: ensgd1@bath.ac.uk

A. J. Rawlinson  
Rolls Royce plc, Derby, UK

### Nomenclature

$d$	hole diameter
$h$	heat transfer coefficient
$I_{\text{actual}}$	actual momentum flux ratio, $= \frac{\rho_c v_c^2}{\rho_m v_m^2}$
$I_{\text{ideal}}$	ideal momentum flux ratio, $= \frac{P_{0c} - P_m}{P_{0m} - P_m}$
$P$	pressure
$w$	hole pitch
$Re_d$	Reynolds number based on hole diameter and mainstream flow conditions, $Re_d = \frac{\rho v d}{\mu}$
$T$	temperature
$v$	flow velocity
$x$	distance downstream from the downstream edge of hole
$y$	height above wall
$z$	distance from centre of central hole

### Greek symbols

$\eta$	film-cooling effectiveness, $\eta = \frac{T_{aw} - T_f}{T_{0c} - T_{0m}}$
$\rho$	density

### Subscripts

0	total, stagnation conditions
aw	adiabatic wall
c	coolant
m	gas, mainstream
mesh	temperature measured on mesh
r	recovery
w	wall

### Abbreviations

<i>console</i>	converging slot-hole
TLC	thermochromic liquid crystals

## 1 Introduction

The use of film cooling to protect surfaces in a gas turbine from high mainstream temperatures is well established. Early applications of film cooling (Weighardt 1943; Seban 1960; Eckert and Drake 1972) utilised tangential slots to produce a uniform film of coolant on

the surface, with minimal mixing between mainstream and coolant flows in order to maximise the effectiveness of the coolant and minimise aerodynamic loss caused by cooling. Straight slots, which are simpler to manufacture than shaped slots (Farmer et al. 1997), have also been investigated (Wang et al. 1996). For application to turbine vanes and blades, slots are impractical as a result of the mechanical strength requirements and are usually replaced by rows of discrete holes (Goldstein et al. 1968) in single or double rows (Ligrani et al. 1992). A large body of research has been devoted to developing arrangements of discrete holes, which provide the most uniform level of cooling. Shaped holes, known as fan-shaped or flared holes have been developed with lateral and sometimes streamwise expansion (Schmidt et al. 1994; Sen et al. 1996; Thole et al. 1996; Gritsch et al. 1997, 1998; Ekkad et al. 1997a, 1997b), which improve lateral spreading of coolant. However, as designs with compound angle injection, or lateral expansion, have approached the level and uniformity of slot film cooling, the aerodynamic loss caused by cooling has also increased, because of inefficient diffusion in the fan and subsequent mixing of the coolant with the mainstream (Day et al. 2000).

The patented (Oldfield and Lock, 1998) *converging slot-hole*, or *console*, has been developed in response to the need for a film-cooling system with the mechanical stability of discrete holes, but with a high film-cooling effectiveness, uniform lateral cooling and low aerodynamic loss. The *console* has been tested at both low speed, incompressible conditions on a flat-plate model (Sargison et al. 2002a) and at engine-representative conditions, on a nozzle guide vane (NGV), in an annular cascade (Sargison et al. 2002b). In these experiments, the *console* performance was compared with discrete cylindrical, laterally expanded holes and a slot, and it was found that the performance was indeed similar to slot flow.

The purpose of the current work is to achieve some understanding of the *console* film-cooling results using flow visualisation. Some of the work in this paper has previously been presented at a conference by Sargison et al. (2002c).

## 2 Console

The *console* design is discussed in Sargison et al. (2002a, 2002b). The cross-section of the *console* changes from a near circular shape at the inlet to a slot at the exit. In the side view (Fig. 1a), the walls of the *console* converge and in plan view (Fig. 1b), the walls diverge, but the convergence is greater than the divergence so that the cross-sectional area decreases and the flow accelerates from the inlet to the outlet. The minimum hole area (throat) and hence the maximum flow velocity are at or close to the hole exit.

Individual holes in a row of *consoles* are positioned such that adjacent holes intersect just below the surface

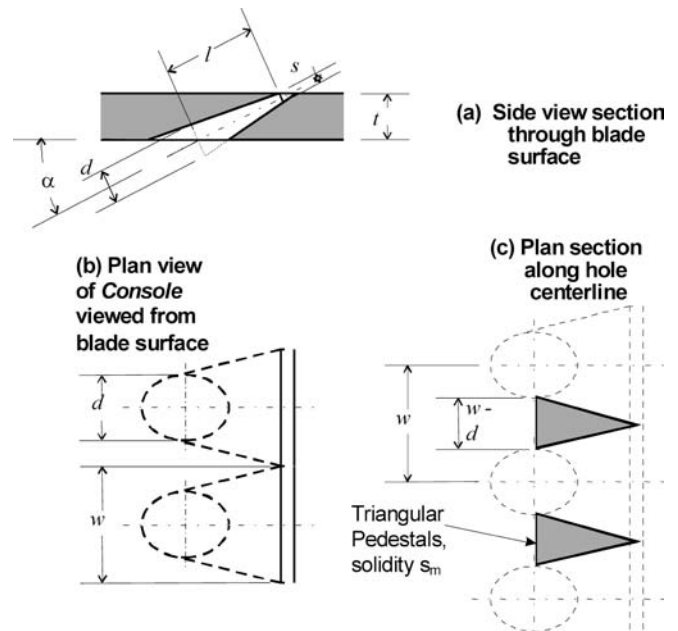


Fig. 1 Basic *console* configuration

as shown in Fig. 2, and a continuous slot is formed on the outside blade surface. The continuous coolant film emitted from the slot will provide more uniform cooling, which should benefit from the Coanda effect (Schlichting 1979) and not lift off from the blade surface. The Coanda effect causes a stream of air (or any fluid) emerging from a nozzle to tend to follow a nearby curved surface, if the curvature of the surface or the angle that the surface makes with the emerging stream is not too sharp. The experiments documented in this paper verify that the jets from the *console* do remain attached to the surface, even at high coolant-to-mainstream momentum flux ratios.

The roughly triangular pedestals between holes (Fig. 1) maintain the strength of the blade. The structural integrity of the different cooling hole shapes can be compared by assessing the percentage of material remaining in the cross-sections of the plate containing the holes. The area remaining in a cross-section is expressed as a percentage of the entire cross-sectional area. The minimum cross-sectional area for the particular *console* design used in the current work is 25%,

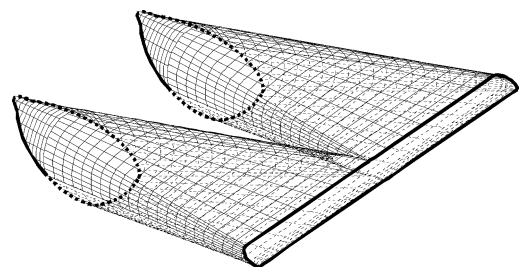
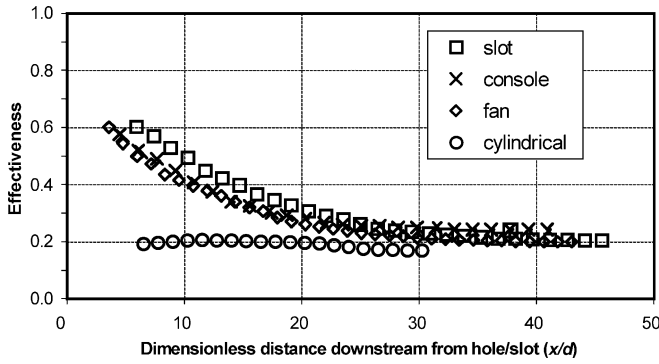


Fig. 2 Unigraphics surface definition of two *console* film-cooling holes



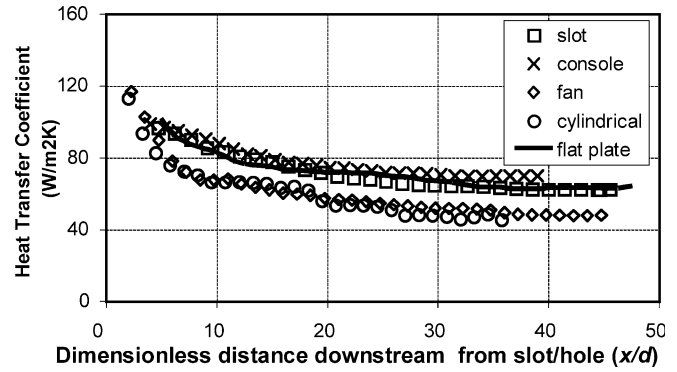
**Fig. 3** Laterally averaged adiabatic effectiveness;  $I_{ideal} = 1.1$ ,  $v_m = 26 \text{ ms}^{-1}$  from Sargison et al. (2002a)

reduced from 52% for the fan-shaped holes, and 67% for the cylindrical holes. The holes were spaced to give throat area per unit width equivalent to a row of cylindrical holes with a  $p/d$  of 3. The residual strength of the material with *consoles* should be sufficient, but further studies of the mechanical design of the *console* are required to verify this.

Published measurements of film-cooling thermal and aerodynamic performance (Sargison et al. 2002a) showed that the *console* provides both high levels of cooling and low aerodynamic loss. The comparison of laterally averaged adiabatic effectiveness and heat transfer coefficient results for the *console* and other typical hole shapes are shown in Figs. 3 and 4 from (Sargison et al. 2002a). Note that the ideal momentum flux ratio,  $I_{ideal}$  is defined as  $(p_{0c} - p_c)/(p_{0m} - p_m)$ . These results compare favourably with data from Eckert and Drake (1972), Sen et al. (1996), Ekkad et al. (1997a, 1997b) and Gritsch et al. (1998). From these results, the *console* exhibits similar cooling to the slot with a high effectiveness, but with a higher heat transfer coefficient than cylindrical and fan-shaped hole film cooling. The explanation for this behaviour was assumed to be the difference in film thickness between the *console*/slot and the cylindrical/fan-shaped hole films, with the cylindrical and fan-shaped hole films assumed to provide a thicker film. A thicker film would tend to provide a reduction in temperature gradient through the boundary layer and, hence, a reduction heat transfer coefficient  $h$ .

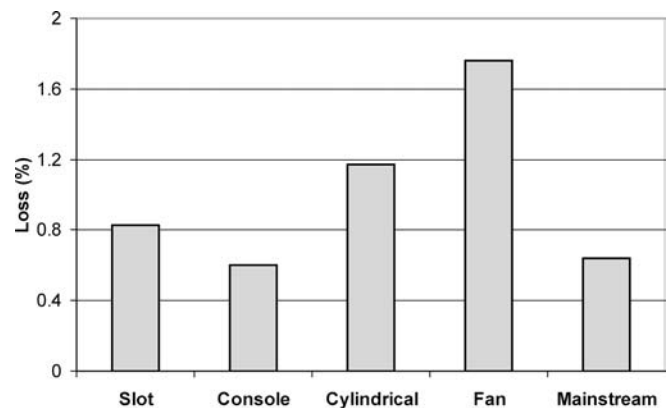
A reduction in heat transfer coefficient in the presence of film cooling might initially appear counter intuitive. The authors note that some researchers have measured  $h$  to be enhanced as a result of cooling. However, the coolant film has two mechanisms: one is to mix with the mainstream flow, which increases  $h$ ; the other is to thicken the boundary layer, which reduces  $h$  as the thermal gradient is reduced. It is the authors' view that in the present situation the boundary layer thickening mechanism is the stronger influence, hence the heat transfer coefficient  $h$  is reduced.

Figure 5 shows the aerodynamic loss measurement based on kinetic energy measurements from a boundary layer traverse downstream of film-cooling injection, from



**Fig. 4** Laterally averaged heat transfer coefficient;  $I_{ideal} = 1.1$ ,  $v_m = 26 \text{ ms}^{-1}$  from Sargison et al. (2002a)

Sargison et al. (2002a). The upstream conditions for the loss calculation were the total pressure of the coolant in the plenum and the mainstream total pressure upstream from injection, in order to take into account the loss through the cooling hole. The most significant benefit of the *console* over traditional film-cooling hole shapes is clearly the low aerodynamic loss due to film cooling. Indeed, the loss with coolant ejection from the *console* is equal, within the bounds of experimental uncertainty, to the loss with no cooling; that is, only the mainstream flow shown in the final column of Fig. 5. The *console* film may re-energise the boundary layer, leading to this low level of aerodynamic loss. The main reason for the superior performance of the *console* would appear to be that the flow through the film-cooling hole is accelerating. Consequently, losses associated with separations and turbulence in non-accelerating hole flows are reduced. It has been widely established (e.g. Schlichting 1979) that for accelerated flows, the boundary layer generally remains laminar or turbulent boundary layers relaminarise while even a small amount of diffusion generally induces transition to turbulent flow. The losses resulting from turbulent flow are significantly higher than for laminar flow. Also, the very thin, attached film flow exiting from the *console* would have reduced interaction with the



**Fig. 5** Comparison of aerodynamic loss of four cooling configurations;  $I_{ideal} = 1.1$ ,  $v_m = 26 \text{ ms}^{-1}$ , uncertainty =  $\pm 0.2\%$

mainstream flow compared with thicker, more diffuse films.

The flow visualisation experiments presented in this paper were developed in order to increase the understanding of the film-cooling flow from a row of *console* film-cooling holes in order to determine the mechanisms controlling *console* performance. The flow visualisation has demonstrated that slot-like flow can be obtained from individual holes. The data presented is primarily used to compare the performance of *console* with the other commonly used geometries and to understand the mechanisms for the low aerodynamic loss. A range of momentum–flux ratios were used: some experiments were conducted at engine-representative conditions; others were chosen to show that the engine designer can achieve slot-like flow from discrete holes that will remain attached even at high momentum–flux ratios.

### 3 Experimental technique

#### 3.1 General apparatus

The experiments were performed in a 500×500 mm cross-section low speed wind tunnel in the Osney Laboratory at the University of Oxford. The mainstream flow speed could be varied and operating speeds of  $5 \text{ ms}^{-1}$  and  $26 \text{ ms}^{-1}$  were used. The freestream turbulence intensity was of the order of 1%. This is significantly less than typical turbulence at engine conditions, however the turbulence was considered satisfactory for the purpose of the current comparative experiments. The total boundary layer thickness at injection was 20 mm or one hole diameter, based on the cylindrical holes tested.

The coolant airflow was supplied from the laboratory compressed air supply and the mass flow rate of air supplied was measured through a British Standard, BS 1042 orifice plate. The air was independently heated using an inline heater before feeding into a plenum chamber located behind the film-cooling hole plate. The coolant-to-mainstream density ratio was nominally one,

but varied owing to the heating of the coolant flow to a minimum of 0.94.

The film-cooling holes were machined in plates that could be easily interchanged between experiments. The plate material was Rohacell type 51G—a closed pore, structural foam, manufactured by Rohm GMBH, with low thermal conductivity of 0.028–0.034 W/mK at 20°C, compared with the air conductivity of 0.025 W/mK. The hole shapes tested were sized to have the same throat area per unit width as a row of 20-mm diameter cylindrical holes at a pitch of  $3d$ . The shapes tested are shown in Fig. 6, and were as follows:

- a row of five cylindrical holes;
- a row of three fan-shaped holes;
- a parallel slot;
- a row of five *consoles*

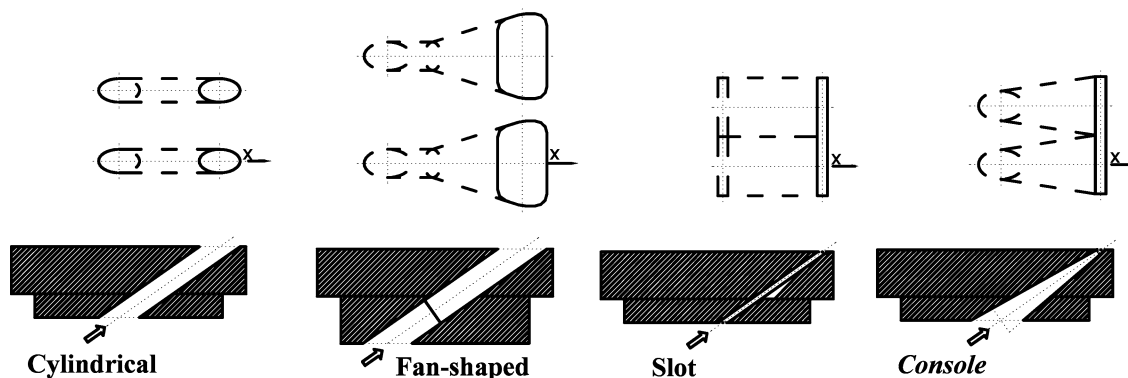
The slot height was 5 mm, the *consoles* had the same slot height at the throat and an inlet diameter of 25 mm. The fan-shaped holes had a cylindrical section diameter of 24 mm, cylindrical section length of  $1.9d$ , total hole length of  $5.8d$ , lateral expansion angle of  $14^\circ$  and a pitch of  $3.5d$ . The cylindrical holes had a diameter of 20 mm, pitch of  $3d$  and a length of  $5.2d$ . All holes were inclined at  $35^\circ$  to the downstream direction.

#### 3.2 Liquid crystal flow visualisation

The first flow visualisation data was collected using a liquid crystal technique, similar to that used by Mee et al. (1999). The fine nylon mesh fabric with low aerodynamic resistance, shown in Fig. 7 was stretched onto a frame constructed from acrylic, which covered the height and half the width of the tunnel test section (Fig. 8). The frame was recessed into the wall of the wind tunnel, so that it did not interfere with the near wall flow, and the join between the frame and the wind tunnel wall was sealed so that there was no flow leakage at the mesh insertion location.

The mesh was sprayed with narrow band TLC, which after calibration provided an uncertainty in adiabatic effectiveness of  $\pm 5\%$ . The TLC were calibrated using two thin-wire, K-Type thermocouples threaded into the mesh. The calibration was conducted in situ under lighting conditions and camera-viewing

Fig. 6 Typical film-cooling hole configurations



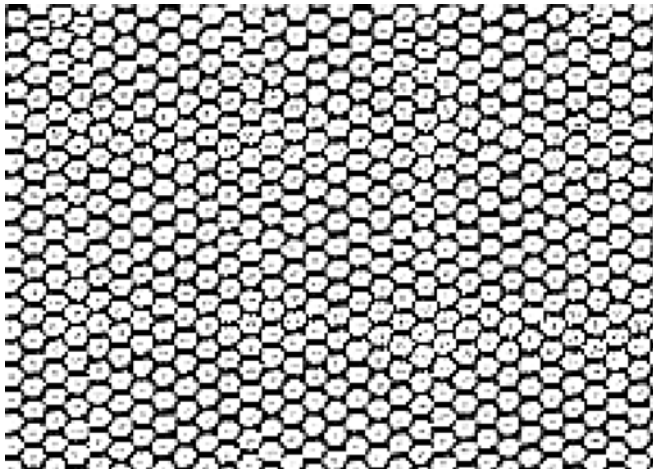


Fig. 7 Nylon mesh fabric (cells ~2 mm in width, fibre <0.2 mm)

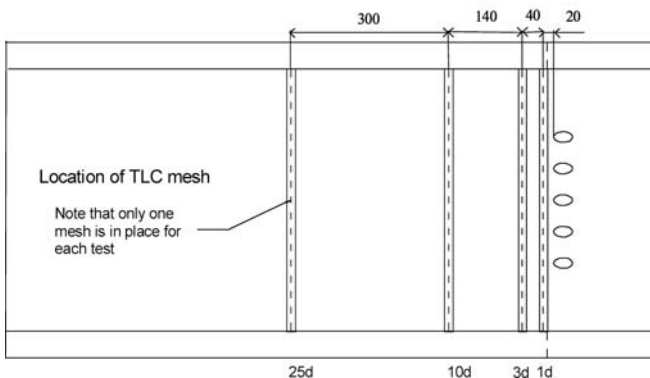
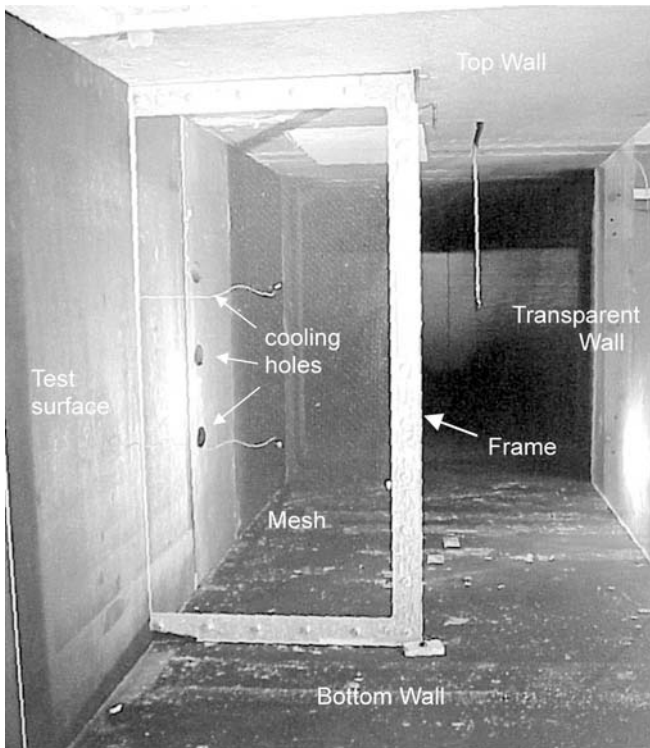
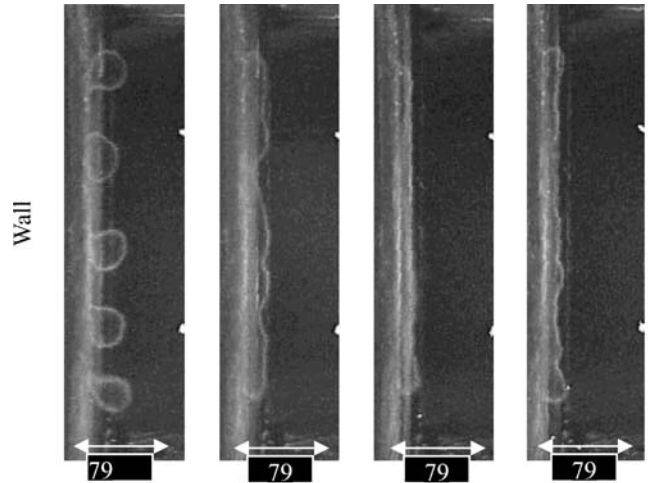
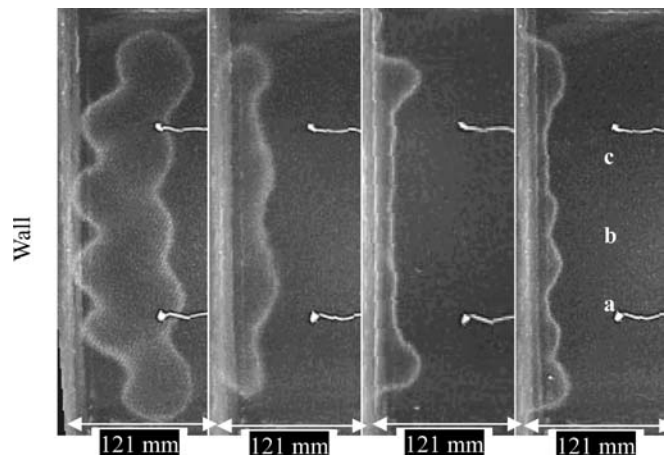


Fig. 8 Locations of mesh in wind tunnel. *Top*: photograph of the mesh screen in the tunnel viewed from downstream. *Bottom*: plan view of the mesh positions



Cylindrical (5 jets) Fan-Shaped (3 jets) Slot; Console (5 jets)

Fig. 9 Photographs of contours at  $10d$ , with  $I=1.1$  and  $v_m=26 \text{ ms}^{-1}$



Cylindrical (5 jet); Fan-Shaped (3 jet); Slot; Console (5 jet)

Fig. 10 Photographs of contours at  $10d$ , with  $I=40$  and  $v_m=5 \text{ ms}^{-1}$

angles identical to that used in the experiment. The flat-plate wall of the wind tunnel was adapted such that the mesh could be inserted at distances of 1, 3, 10 and 25 cylindrical hole diameters from the film-cooling hole exit. The wind tunnel working section was painted black on the top, floor and one side-wall to provide a good contrast for the liquid crystal images. The remaining side-wall was constructed from acrylic to provide visual access to the working section, which was lit by two low-temperature halogen lights mounted in fixed locations.

A digital camera was mounted in the wind tunnel, well downstream of the mesh, in order to record images of the crystal colour play at various coolant temperatures. A set of experiments was conducted to match the low speed experiments documented in Sargison et al. (2002a), with a mainstream speed of  $26 \text{ ms}^{-1}$  (Reynolds number of 36,000, based on mainstream flow and

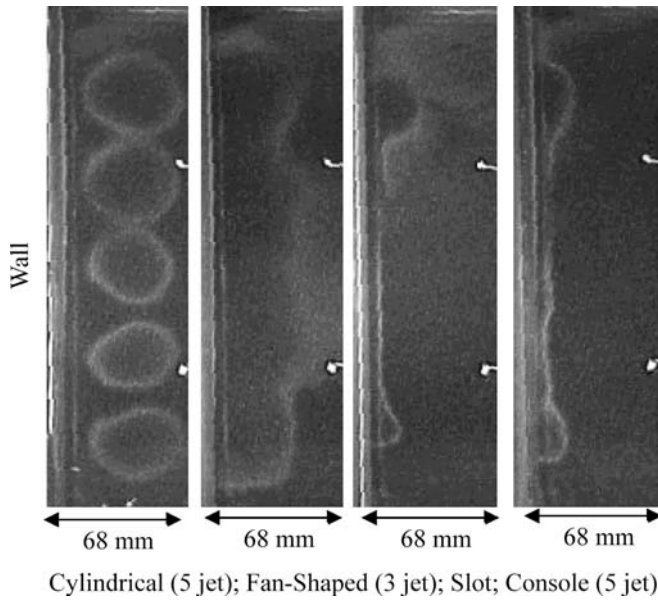


**Fig. 11** Photographs of contours at  $3d$ , with  $I = \infty$  and  $v_m = 0 \text{ ms}^{-1}$

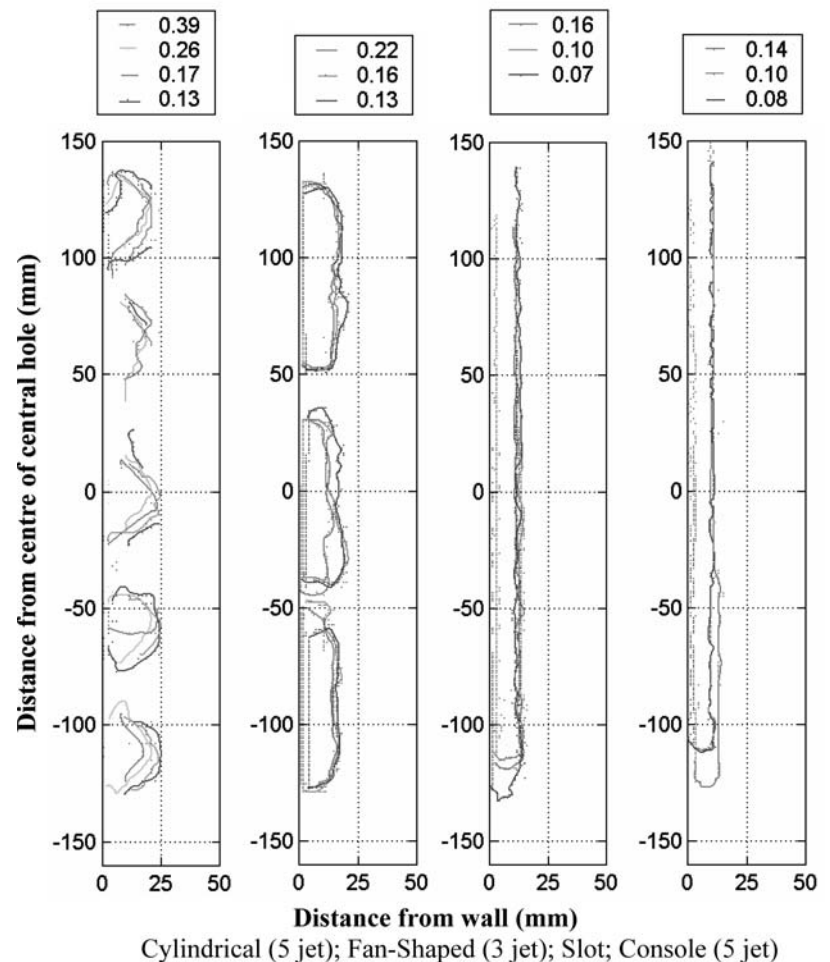
cylindrical hole diameter) and ideal momentum flux ratio (based on driving pressures) of 1.1. The nominal density ratio of 1 for the experiments, produced a

blowing ratio close to 1 for  $I_{\text{ideal}} = 1.1$ . Each contour of effectiveness was generated by adjusting the coolant temperature, and the contours were moved as the coolant temperature was changed.

In order to test whether the *console* flow benefited from the Coanda effect, the experiments were also conducted with a low mainstream speed of  $5 \text{ ms}^{-1}$  (Reynolds number of 6,000), and without crossflow. For both these cases, the coolant driving pressure,  $P_{0c} - P_m$ , was kept constant at the design crossflow ( $Re = 36,000$ ) level, resulting in an ideal momentum flux ratio of 40 for the low mainstream speed and an infinite momentum flux ratio for the case without crossflow. The purpose of expanding the experimental regime to these uncharacteristic momentum flux ratios was to test that the *console* does indeed provide engine designers with the opportunity to have slot-like flow issuing from discrete holes.

The temperature measured using this technique was the temperature of the mesh fibres. The thermal conductivity of the fibres and the temperature gradients along them were low, so that the conductive heat transfer along the net was negligible compared with the heat convected from the flow. The mesh fibres were very fine ( $< 0.2 \text{ mm}$ ) and the blockage caused by the mesh in the flow was negligible compared with the accuracy of

**Fig. 12** Contours of effectiveness at  $1d$ ,  $I = 1.1$ ,  $\Delta P_c = 412 \text{ Pa}$ ,  $v_m = 26 \text{ ms}^{-1}$



the experiment. Mee et al. (1999) found that the error in jet contour location caused by broadening of the jet due to the blockage of the mesh was less than 5% at 40 jet diameters. The acrylic frame is distant from the measured surface flow and did not perceptibly disturb it. The spatial resolution of measurements made using the mesh was the mesh cell size of 2 mm.

The uncertainties in measured data presented are as follows:

- adiabatic effectiveness:  $\pm 5\%$
- momentum flux ratio:  $\pm 1\%$
- contour location:  $\pm 2$  mm

#### 4 Liquid crystal measurement technique

The images of the liquid crystal colour play, such as those shown in Figs. 9, 10 and 11, were enhanced in Matlab (The MathWorks Inc., Natick, MA, USA) using the blue part of the RGB data. The edges of the TLC colour play and, hence, the temperature contours, were extracted from the regions of highest colour gradient. An attempt was made to produce a full set of contours across the flow

field, but it was found that while the results are useful for the purpose of gaining an understanding of the thermal flow field, the contours are not of suitable quality to be interpolated over the flow field. This is because the use of narrow band TLC produces a set of contours recorded at different times, with the accompanying problem of movement of contours owing to the flow unsteadiness and spatial resolution. The use of wide band TLC would allow an instantaneous set of contours to be collected, but would introduce more complication in the system calibration. In addition, this would not highlight the true nature of the jets, which are unsteady, and the location of the contours varies with time.

In addition to providing a qualitative of the size and shape, and location of the film-cooling jets at constant coolant temperature, the TLC mesh technique produced quantitative contours of gas effectiveness. The gas effectiveness is defined similarly to wall adiabatic effectiveness (Sargison et al. 2002a), with the temperature at the mesh replacing the adiabatic wall temperature:

$$\eta_{\text{gas}} = \frac{T_{\text{mesh}} - T_r}{T_{0c} - T_{0m}} \quad (1)$$

**Fig. 13** Contours of effectiveness at  $3d$ ,  $I=1.1$ ,  $\Delta P_c=412$  Pa,  $v_m=26$  ms<sup>-1</sup>

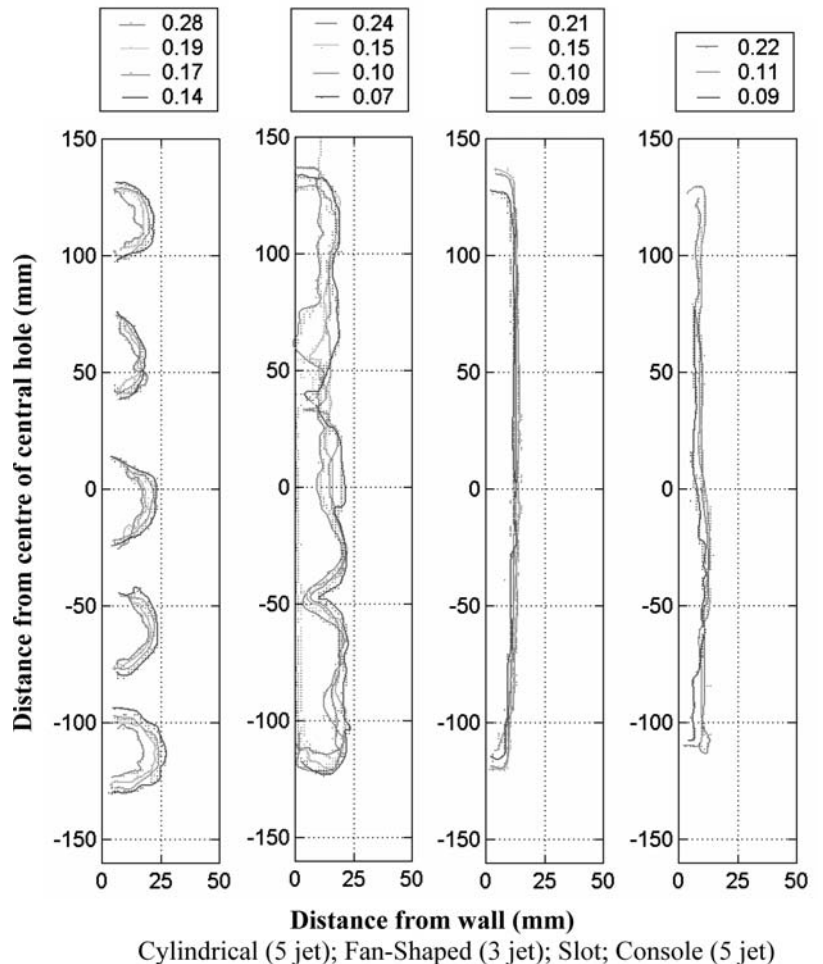
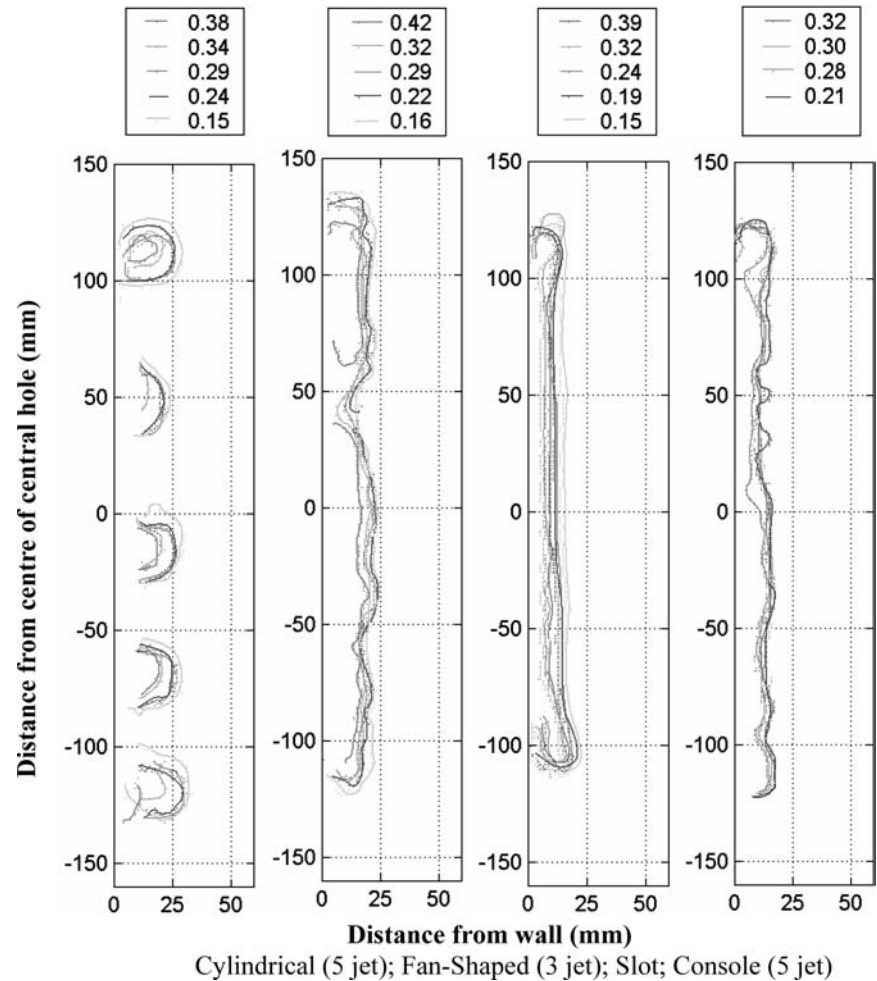


**Fig. 14** Contours of effectiveness at  $10d$ ,  $I=1.1$ ,  $\Delta P_c=412$  Pa,  $v_m=26$  ms<sup>-1</sup>



## 5 Liquid crystal experimental results

Figures 9 and 10 show the liquid crystal images at a distance of  $10d$  from injection with  $v_m=26$  ms<sup>-1</sup> and  $v_m=5$  ms<sup>-1</sup>, respectively. The images shown are at the highest coolant temperature, giving a gas effectiveness of approximately 0.1 along the displayed TLC lines.

In Fig. 9 (design  $Re_d=36,000$ , design  $I$ ), the *console* and slot films are shown to have a similar thickness. The *console* film shows some structure, or non-uniformity, compared with the slot owing to the five discrete holes in the *console* row. The fan-shaped hole film is thicker than the slot and *console* films, and the jet structure from the three fan-shaped hole jets is visible. The jets are closer to the surface downstream of the hole centre. The cylindrical hole film is significantly thicker than the other films, and the five jets do not meet. The jets at the edge of the row have almost lifted off the surface in this view. In this and the following figures it is clear that there is some interaction between the outer jets, or the outer region of the slot and *console* flows and the mainstream flow at the outer edges of the coolant flow. This has the effect of lifting the jets further from the surface than is typical for the quasi two-dimensional mainstream flow

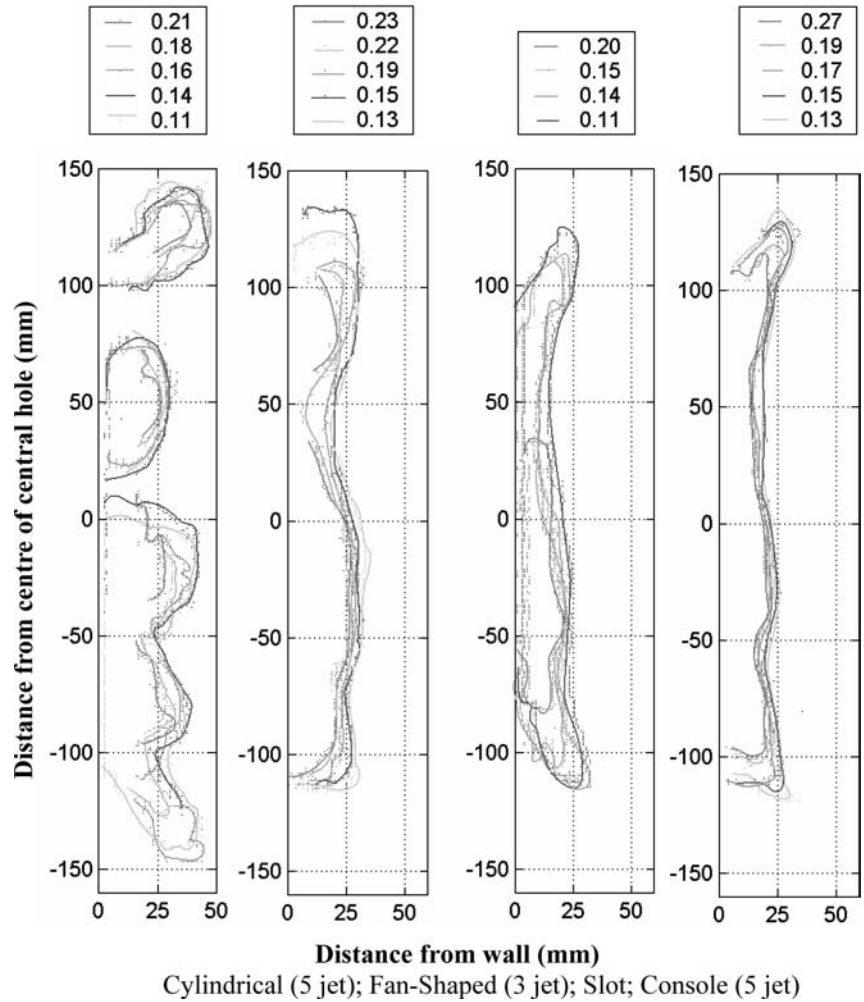
over the central jets. This feature is included in these results, but the laterally averaged effectiveness, heat transfer and loss results presented in Figs. 3, 4 and 5 are produced from the central holes only.

In Fig. 10 with a much lower mainstream  $Re_d$  (6,000), all of the jet features mentioned can be very clearly identified. The cylindrical jets have lifted off the surface at the jet centre. The fan-shaped hole structure is similarly clear. The slot flow remains very uniform, except at the edges of the slot, where wall vortices cause the jet to spread out from the surface. The *console* film shows that the two edge jets spread from the surface and the two lower jets (marked a and b) exhibit structure, with the centre of the jet pressed towards the surface.

The structure observed in the film produced by the *console* jets is demonstrated by the varying thickness of the film, and by regions of higher effectiveness downstream of the point where adjacent film-cooling holes join (as identified by Sargison et al. 2002a). It is likely that this structure is due to the interaction between jets issuing from adjacent holes. This interaction is most significant in the case of *console* because the holes are immediately adjacent to each other. This differs from the case of fan-shaped holes, where a short separation dis-



**Fig. 15** Contours of effectiveness at  $25d$ ,  $I = 1.1$ ,  $\Delta P_c = 412$  Pa,  $v_m = 26$  ms<sup>-1</sup>



tance exists, in that they display jet interaction a distance downstream from the hole exits.

Increased uniformity is demonstrated by the jet marked c in the photograph. The *console* upstream of this jet has been shaped prior to the experiment by radiusing both the inlet and outlet edges of the hole. This indicates that there should be an advantage in shaping the holes, because the film becomes more similar to the slot film.

The images in Fig. 11 show the jets with no crossflow. The cylindrical jets lift completely off the surface and the fan-shaped hole film is very thick and diffused near the edges of the jet, although it does remain attached to the surface. The *console* and slot films both demonstrate the Coanda effect, because they remain attached to the surface. Again, there is some structure in the *console* jet and the film is completely removed from the surface for the two edge holes. This indicates that the slot-like flow characteristics exhibited by the *console* are dependent on the interaction between adjacent *consoles*. A single console would act more like a discrete cylindrical hole, with jet detachment from the surface. It is only when consoles are placed in a row, with individual holes

merging at exit, that the slot performance is achieved. At distances further downstream ( $10d$  and  $25d$ ), the jets were not as well defined because the warm jet was mixed with the cool ambient air and the edge contour was difficult to extract.

### 5.1 Effectiveness contours with crossflow: design conditions

The gas effectiveness contours in Figs. 12, 13, 14 and 15 are for the case of a mainstream-velocity crossflow of 26 m/s, a design Reynolds number ( $Re_d = 36,000$ ) and ideal momentum flux ratio ( $I_{ideal} = 1.1$ ). These figures illustrate the development of the jet flow with downstream distance from the injection point. The range of gas effectiveness that could be measured was limited by the mesh crystal temperature and the maximum coolant temperature available. It was not possible to measure gas effectiveness very close to the wall because of the difficulties in viewing the mesh with the camera. The emerging coolant for all geometries tested featured a core of high gas effectiveness with a strong gradient in

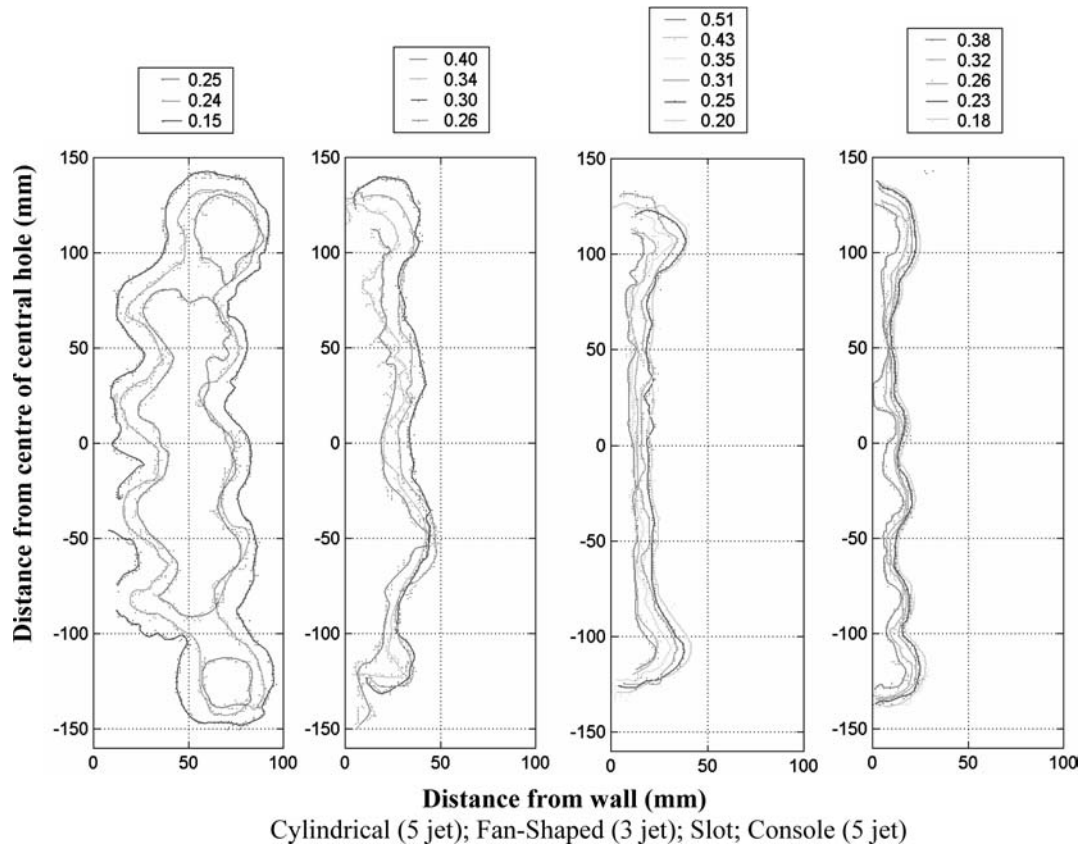


**Fig. 16** Contours of effectiveness at  $10d$ ,  $I=40$ ,  $\Delta P_c = 412$  Pa,  $v_m = 5$  ms<sup>-1</sup>

temperature at the edges of the jets. Thus the contours of low effectiveness in Figs. 12, 13, 14 and 15 are closely spaced and identify the extent to which the coolant penetrates the mainstream.

The edges of the coolant jet emerging from the slot and *console* are observed to remain close to the surface, indicating a continuous film of high gas effectiveness at the wall. At  $25d$ , the jets are diffused and at the boundaries (top and bottom of the figures) the film begins to separate from the surface. The region of the coolant jet away from the jet boundary remains attached and uniform. The fan-shaped hole jets are separate close to the hole, but they spread to form a closed film from  $3d$  downstream. At  $25d$ , the film is continuous, with some small structure from the fan jet vortices. The fan film is thicker than the slot and *console* films at all downstream distances. The cylindrical jets do not meet and remain at a similar thickness until  $25d$ , where the film thickness has increased significantly and the lower three jets have joined. The jets at the top and lower boundaries also start to lift off the surface.

The increased thickness of the fan-shaped and cylindrical hole coolant films cause the reduction in heat transfer coefficient observed in Fig. 4. The shape of the coolant film will also affect the aerodynamic efficiency of film cooling. The slot and *console* films are very uniform and do not penetrate significantly into the flow. In fact,

the film thickness for the slot and *console* is similar to the boundary layer thickness with no film cooling. Hence, the measured aerodynamic loss for both the slot and *console* films was low, and similar to the level without cooling (Fig. 5 and Sargison et al. (2002a)). In contrast, the film formed by cylindrical and fan-shaped hole film cooling has increased penetration into the mainstream, and the spreading of effectiveness contours indicates diffusion and mixing of the coolant film with the mainstream. This disturbance and mixing caused by cooling with fan-shaped and cylindrical hole jets will increase the aerodynamic loss as a result of processes external to the hole.

## 5.2 Effectiveness contours with low crossflow:

$v_m = 5$  ms<sup>-1</sup> and  $I=40$

Experiments were conducted at the same coolant momentum flux as those discussed above, but with a mainstream flow of low velocity. Although not typical of engine designs, this high momentum flux ratio provides exaggerated conditions to test the slot-like behaviour of a row of consoles, and the jet shapes are more pronounced than the design case. The gas effectiveness contours for these experiments are shown in Figs. 16 and 17. Note that, with reference to Figs. 12, 13, 14 and 15, the horizontal scale denoting distance from the wall has been expanded. With low velocity crossflow and, hence, high coolant-to-mainstream momentum flux ratio, the jet interaction with the mainstream flow is

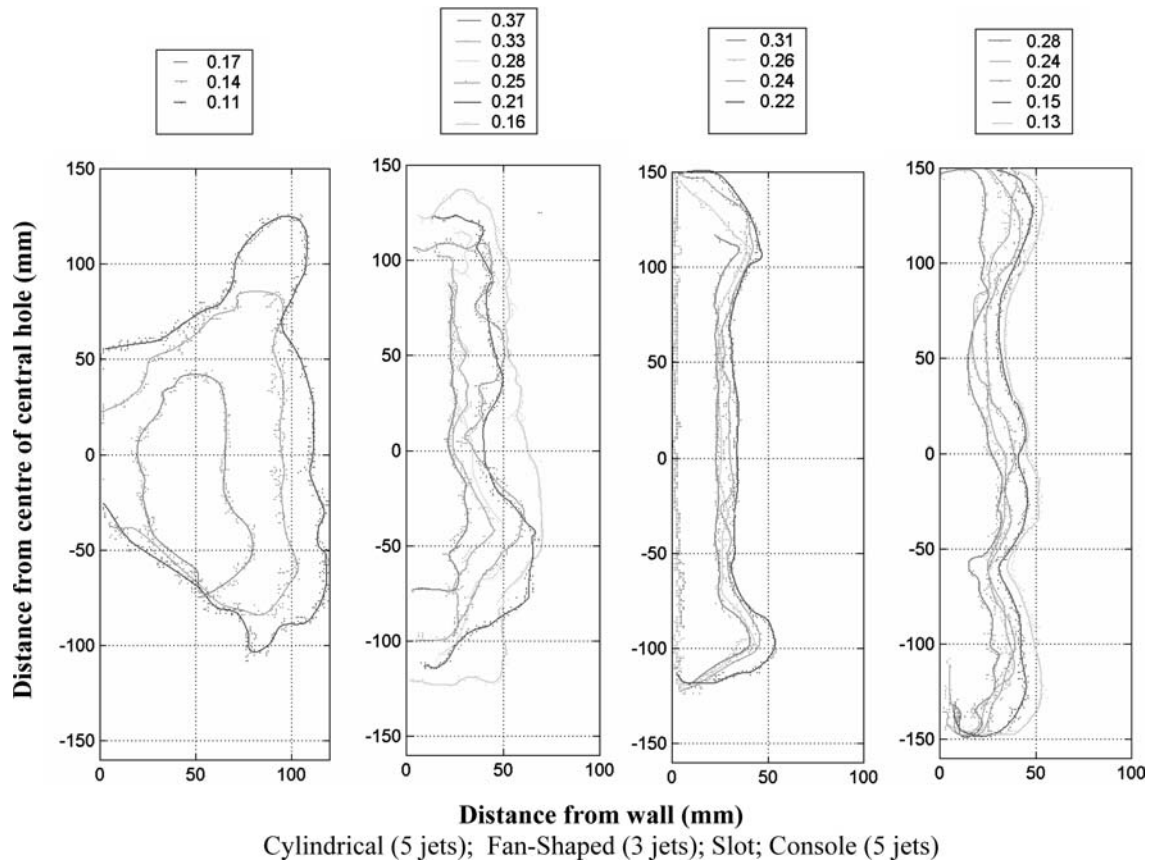


**Fig. 17** Contours of effectiveness at  $25d$ ,  $I=40$ ,  $\Delta P_c=412$  Pa,  $v_m=5$  ms<sup>-1</sup>

significantly more apparent than for the previous cases. Evidence of the jet vortex structure is apparent in Fig. 16, at  $10d$ , but in Fig. 17, at  $25d$ , the jets have become diffused. The cylindrical jets have mixed with the mainstream to form a single mass of coolant in which patterns are not distinguishable using this technique. The crossing of contours in some figures is a result of the unsteadiness of the coolant jets interacting with the mainstream flow. Each contour was measured at a different time after the effectiveness was adjusted by variation of the coolant temperature. At very low effectiveness (high coolant temperature), some buoyancy is apparent in the jets, which are skewed slightly towards the top of the wind tunnel.

The slot flow remains uniform and close to the surface, and the *console* flow again exhibits some structure, but remains very close to the surface. In these conditions, the differences between the cylindrical and fan-shaped hole film cooling and the *console* and slot are more exaggerated, but remain in the same trend as the previous results. For the slot and *console* the adiabatic effectiveness will be high and uniform and the aerodynamic loss low, because of the thin, uniform film. The cylindrical and fan-shaped hole films have high aerodynamic loss, but a low heat transfer coefficient because of the thicker, more diffuse film.

### 5.3 Contours with no crossflow

The slot film is extremely uniform without crossflow, as might be expected, except for near the edges of the slot (see Figs. 18 and 19). Here, the coolant formed a thicker layer, presumably because of vortices formed at the edge of the jet, although it did not lift off from the surface. For the *console* coolant film without crossflow, the jets from the two outside edge holes lifted off from the surface. This was interesting because it reinforces the fact that one of the strong advantages of the *console* is the interaction of jets from adjoining holes. An individual *console* would not benefit as much from the Coanda effect and would remain attached to the surface at very high blowing rates or without crossflow.

The cylindrical jets lifted off the surface and the spacing of the effectiveness contours show that there was more mixing of the jet with ambient air, causing the jet boundaries to be more diffused. The fan-shaped hole film again remained attached to the surface, but in a film that was quite diffused near the edge and was spread almost to the thickness of the cylindrical jets.

## 6 Water/dry-ice fog flow visualisation

Flow visualisation experiments were also conducted using a water droplet fog. The high-volume coolant flow makes it difficult to obtain sufficient smoke density with

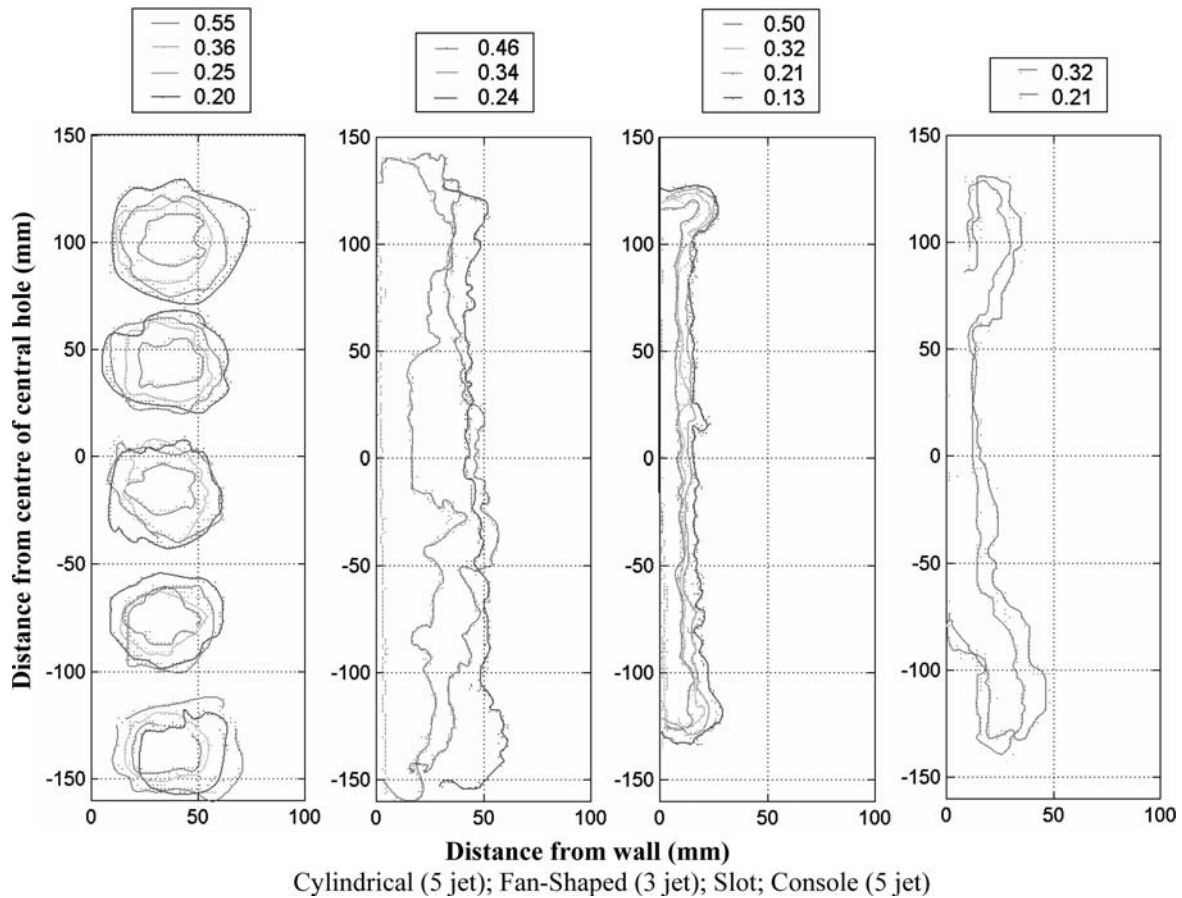


**Fig. 18** Contours of effectiveness at  $1d$ ,  $I=\infty$ ,  $\Delta P_c=412$  Pa,  $v_m=0$  ms $^{-1}$

conventional hot oil smoke generators and so a high density fog generator, such as that used for special effects, was developed. Further details are available in Mann (2002). The technique is limited in the sense that it can only provide qualitative flow visualisation. However, the results are useful as they qualitatively support the time-averaged flow features captured by the liquid crystal images. In addition, the use of flash photography has given an indication of the unsteadiness of the flow for all four cooling configurations.

Dry ice (frozen carbon dioxide) was placed in a reservoir in the coolant supply line. When solid carbon dioxide ( $\text{CO}_2$ ) is dropped into hot water, the water appears to boil. This is not the case, however, as the water remains below  $100^\circ\text{C}$ . The bubbling and agitation is the result of solid  $\text{CO}_2$  turning into a gas. A large amount of white fog is produced during this reaction. The smoke is not  $\text{CO}_2$  gas, which is colourless, but water droplets condensing on cold  $\text{CO}_2$  molecules, forming fine water droplets and, hence, the dense white fog, ideal for photographic flow visualisation.

For these experiments, the flow was recorded using short duration flash illumination and a digital camera. Photographs for the flow through cylindrical and fan-shaped holes, the slot and *console* are shown in

Figs. 20a–d, respectively, for  $I=1.1$ . The photographs show an overhead view (main portion of the figure) and side view, obtained using a mirror, at the top of the figures. The triangular shadow at the top left of each image is a lighting artefact and should be ignored.

The flow patterns from the TLC and mesh at  $x/d=1$  (left) and  $x/d=25$  (right) are also shown in each figure. All the discussion in Sect. 5.1 is relevant in describing Figs. 20a–d. It can be seen that the fog flow visualisation confirms the time-averaged flow shown in the liquid crystal images. In addition, the use of a flash has given a strong indication of the unsteadiness of the flow for all four cooling configurations.

In Fig. 20a, the flow from the cylindrical holes shows large-scale eddies, with the lowest holes coalescing to form an even larger eddy. The side view confirms the significant thickness of this mixing layer. Such unsteadiness helps explain the high losses and low cooling performance of such holes. In Fig. 20b, the fanned shaped holes give rise, as expected, to a more even distribution of coolant across the flow, but large-scale eddies are still observed, and there is a suggestion that the fans are not running full.

By contrast, the slot in Fig. 20c shows a much smoother flow near the exit of the hole, along with an apparent laminar to turbulent transition indicated by the vertical black dashed line. The thickness of the coolant layer is less than for the cylindrical and fanned hole

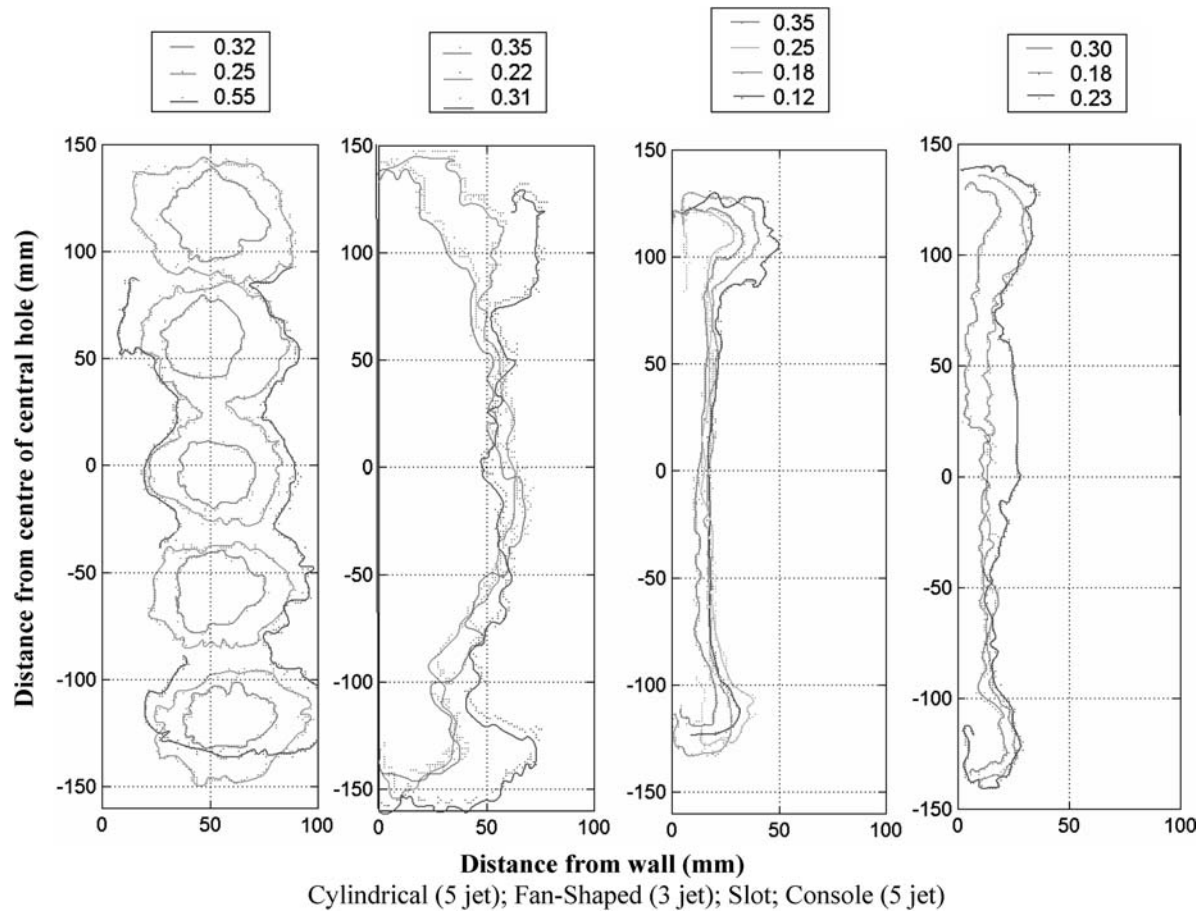


**Fig. 19** Contours of effectiveness at  $3d$ ,  $I=\infty$ ,  $\Delta P_c=412$  Pa,  $v_m=0$  ms<sup>-1</sup>

geometries, and the unsteadiness is of a smaller scale. The *console* in Fig. 20d shows, as had been hoped, a slot-like flow, with only a slight indication of the flow from individual holes. The coolant layer is as thin as that from the slot and the flow structure is similarly of small scale. The apparent transition appears earlier, probably triggered by the internal flow structure. The fog flow visualisation clearly helps explain the superior performance of the console geometry.

## 7 Conclusions

Flow visualisation measurements have been made to investigate the fluid mechanics of coolant ejection from the *console* geometry, as well as from cylindrical holes, fan-shaped holes and a simple slot. Thermal field measurements are presented at 1, 3, 10 and 25 cylindrical hole diameters downstream from injection, at engine-representative conditions ( $Re_d=36,000$ ,  $I=1.1$ ), with reduced crossflow ( $Re_d=6,000$ ,  $I=40$ ) and no crossflow (effectively infinite  $I$ ).

The experiments revealed that the *console* and slot exhibited similar coolant trajectories, which remained attached to the surface even at infinite coolant-to-

mainstream momentum flux ratios. In contrast, the cylindrical hole and fan-shaped hole jets produced diffuse jets of two to three times the thickness of the slot and *console* jets. The cylindrical hole jets lifted off the surface for ideal momentum flux ratios of greater than 1.1. The fan-shaped hole jets were always attached to the surface, but were diffuse at ideal momentum flux ratios above 1.1.

Flow visualisation experiments using water/dry-ice fog show clearly that the flow through all coolant geometries is unsteady, but that the unsteadiness is less for the console and slot geometries.

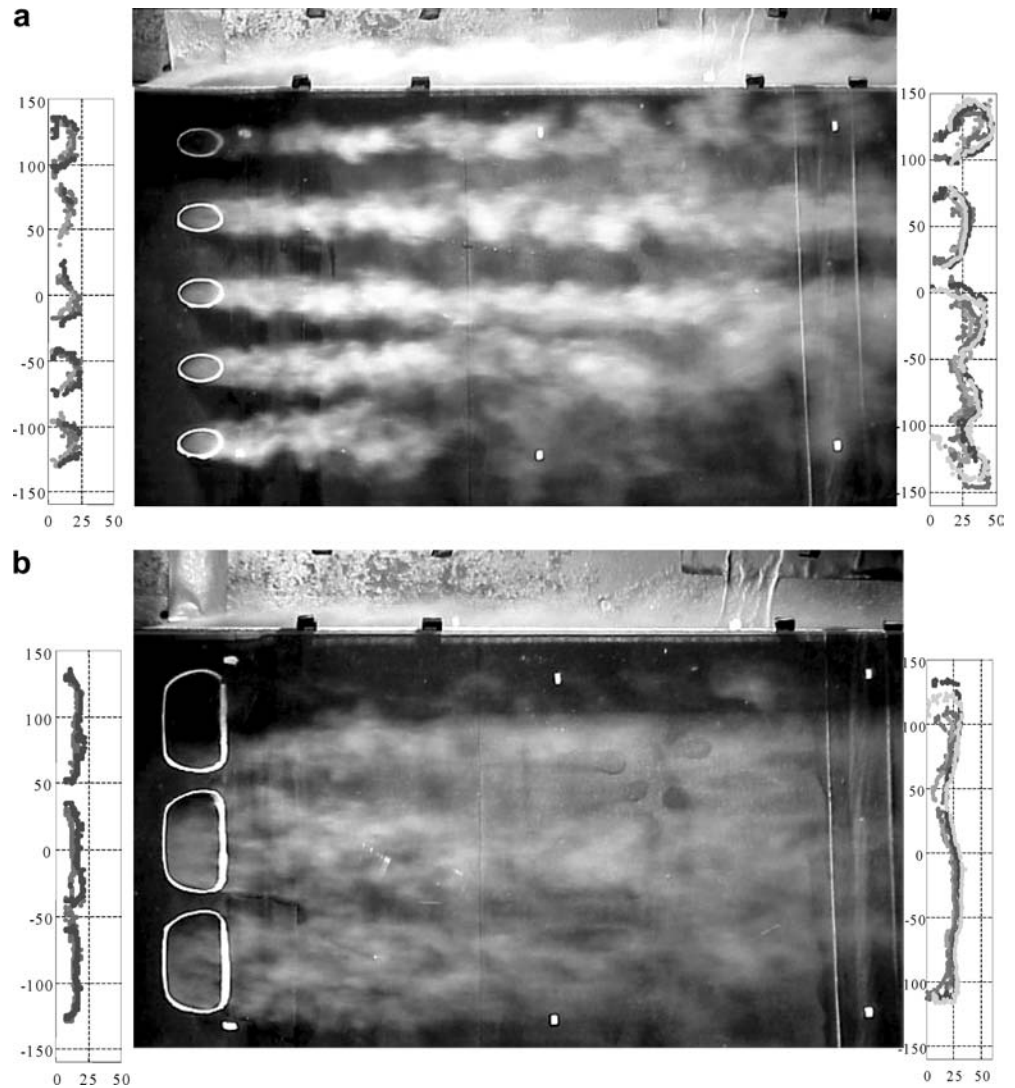
These measurements help explain the enhanced cooling performance and greater aerodynamic efficiency of the *console* over the more traditional cooling geometries.

**Acknowledgements** This work is supported by Rolls Royce plc, QinetiQ, DTI CARAD and MOD ARP26c. The authors also thank Colin Mann for permission to include his fog visualisation images.

## References

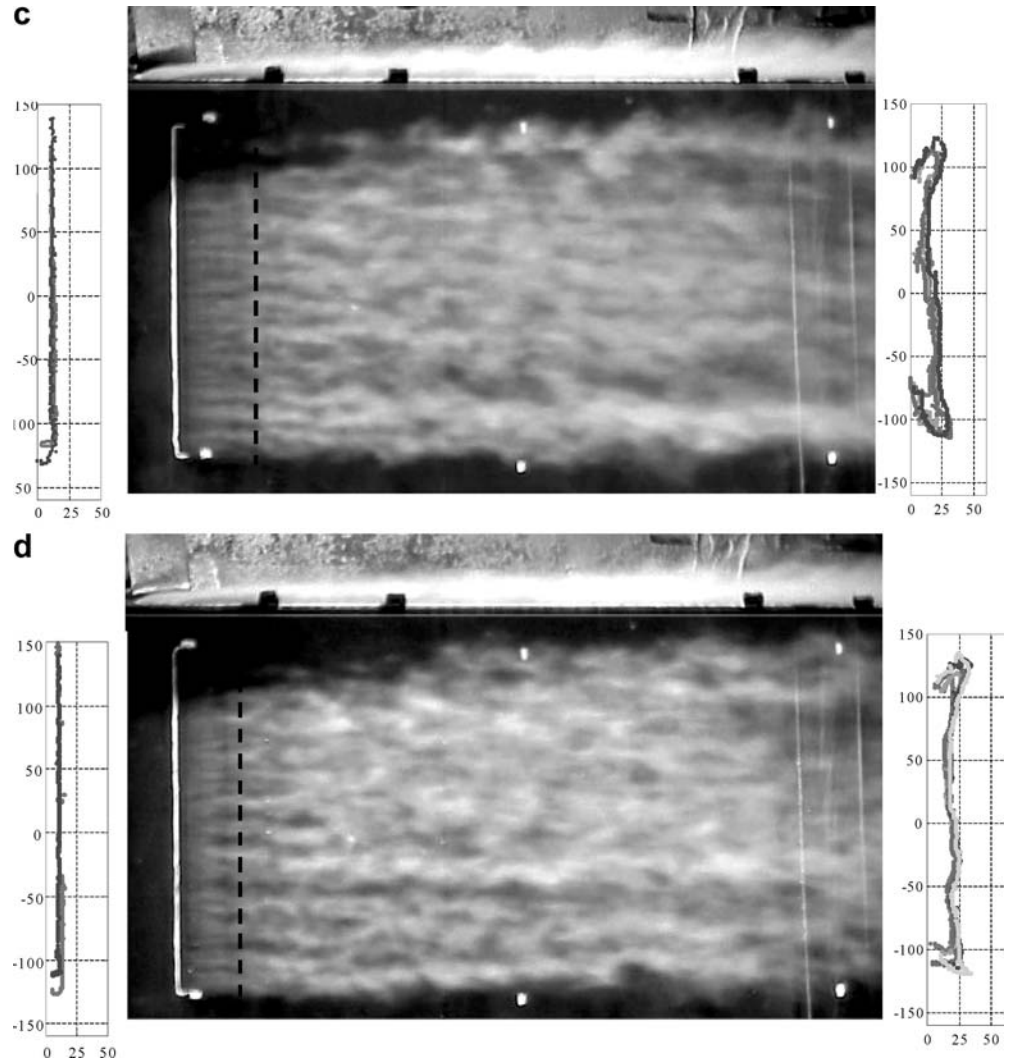
- Day CRB, Oldfield MLG, Lock GD (2000) Aerodynamic performance of an annular cascade of film cooled nozzle guide vanes under engine representative conditions. *Exp Fluids* 29:117–129

**Fig. 20a–d** Flow visualisation photographs with  $I = 1.1$  and  $v_m = 26 \text{ ms}^{-1}$  for: **a** cylindrical holes; **b** fan-shaped holes; **c** slot; **d** console



- Eckert ERG, Drake RM (1972) Analysis of heat and mass transfer. McGraw Hill, New York, pp 453–466
- Ekkad SV, Zapata D, Han JC (1997a) Heat transfer coefficient measurement over a flat surface with air and  $\text{CO}_2$  injection through compound angle holes using a transient liquid crystal method. *J Turbomach* 119:580–586
- Ekkad SV, Zapata D, Han JC (1997b) Film effectiveness measurement over a flat surface with air and  $\text{CO}_2$  injection through compound angle holes using a transient liquid crystal method. *J Turbomach* 119:587–592
- Farmer JP, Seager DJ, Liburdy JA (1997) The effect of shaping inclined slots on film cooling effectiveness and heat transfer coefficient. ASME Paper 97-GT-399
- Goldstein RJ, Eckert ERG, Ramsey JW (1968) Film cooling with injection through holes: adiabatic wall temperatures downstream of a circular hole. *J Eng Power* 90:384–395
- Gritsch M, Schulz A, Wittig S (1997) Discharge coefficient measurements of film cooling holes with expanded exits. ASME Paper 97-GT-165
- Gritsch M, Schulz A, Wittig S (1998) Adiabatic wall effectiveness measurements of film cooling holes with expanded exits. *J Turbomach* 120:549–556
- Ligrani P, Ciriello S, Bishop DT (1992) Heat transfer, adiabatic effectiveness and injectant distributions downstream of a single row and two staggered rows of compound angle film-cooling holes. *J Turbomach* 114:687–700
- Mann C (2002) Flow visualisation of turbine blade film cooling. Final year project report, Department of Engineering Science, University of Oxford
- Mee DJ, Ireland PT, Bather S (1999) Measurement of the temperature field downstream of simulated leading-edge film-cooling holes. *Exp Fluids* 27:273–283
- Oldfield MLG, Lock GD (1998) Coolant passages for gas turbine components, UK patent application no. 9821639.3 (1998) for the new *Console* converging slot hole turbine film cooling hole geometry, University of Oxford, Oxford, UK
- Sargison JE, Guo SM, Oldfield MLG, Lock GD, Rawlinson AJ (2002a) A converging slot-hole film-cooling geometry. Part 1: low speed flat-plate heat transfer and loss. *J Turbomach* 124:453–460
- Sargison JE, Guo SM, Oldfield MLG, Lock GD, Rawlinson AJ (2002b) A converging slot-hole film-cooling geometry. Part 2: transonic guide vane heat transfer and loss. *J Turbomach* 124:461–471
- Sargison JE, Guo SM, Oldfield MLG, Lock GD, Rawlinson AJ (2002c) Flow visualisation of a converging slot-hole film-cooling geometry, ASME Paper GT-2002-30177
- Schlichting H (1979) Boundary-layer theory, 7th edn. McGraw-Hill, New York
- Schmidt DL, Sen B, Bogard DG (1994) Film cooling with compound angle holes: adiabatic effectiveness. ASME Paper 94-GT-312

Fig. 20a–d (Contd.)



Seban RA (1960) Heat transfer and effectiveness for a turbulent boundary layer with tangential fluid injection. *J Heat Transfer* 82:303–312

Sen B, Schmidt DL, Bogard DG (1996) Film cooling with compound angle holes: heat transfer. *J Turbomach* 118:800–806

Thole K, Gritsch M, Schulz A, Wittig S (1996) Flowfield measurements for film-cooling holes with expanded exits. *J Turbomach* 118:327–336

Wang Z, Ireland PT, Kohler ST (1996) Gas temperature measurement in internal cooling passages. ASME Paper 96-GT-534

Weighardt K (1943) Hot air discharge for de-icing (in German). ATI 24536 (original in Dt Luftfahrtforsch Forschungsber)